International Core Journal of Engineering Volume 8 Issue 8, 2022
ISSN: 2414-1895 DOI: 10.6919/ICJE.202208_8(8).0032

Influence of Heating Rate on Giant Stress Impedance Effect of Fe-Based Alloy Ribbons

Huiya Yang[1, a], Fuli Kuang[1], Zheng Fang[4], Jianqiang Zhang[1,3], Yanjun Qin[1,2], Yunzhang Fang[1, *]

[1] Department of Physics, Zhejiang Normal University, Jinhua 321004, China

[2] School of Science, Xinjiang Institute of Technology, Aksu 843100, China

[3] School of Electronic Information and Electrical Engineering, Tianshui Normal University, Tianshui 741000, China

[4] Tourism College of Zhejiang, Hangzhou 311231, China

[a]yanghya@163.com, [*]fyz@zjnu.cn

Abstract

The influence of various heating rates on the giant stress impedance effect of ribbons made of the Fe-based ($Fe_{73.5}Cu_1Nb_3Si_{13.5}B_9$) alloy at 873.15K annealing temperature was examined in this work. Longitudinal drive test for giant stress impedance effect of samples using HP4294A. Significant differences exist in the stress impedance properties. According to the experimental findings, Fe-based alloy strips heated to 873.15K at a rate of 0.17K/s have a material stress impedance ratio of up to 868.65% and a stress response sensitivity of up to 37.36%/MPa. The longitudinal drive can achieve higher stress impedance and sensitivity when compared to other test methods.

Keywords

Stress Impedance; Heating Rate; Fe-Based Alloys; Sensitivity.

1. Introduction

The Fe-based alloy materials are used in a variety of devices[1-3]. Due to their outstanding soft magnetic characteristics, such as high magnetic permeability, high resistivity, and low coercivity. For power electronic components to advance in the direction of low energy consumption, downsizing, and high frequency, it is a "dual green" material, which aids in the achievement of the "dual carbon" goal. Most researchers employ various heat treatment techniques to modify the material properties in order to pursue higher sensitivity for sensors and to meet the diverse needs of material properties in various fields.

In 1998, Yang et al. [4] tested the giant magneto-impedance effect (GMI) of $Fe_{73.5}Cu_1Nb_3Si_{13.5}B_9$ by longitudinal driving method. The non-contact mode method can effectively avoid the Joule heat loss caused by the contact impedance between the wire and the ribbon in the lateral drive mode. And in the longitudinal driving test, a magnetization field along the longitudinal direction of the crystal strip will be generated, resulting in a larger giant magneto-impedance, and the sensitivity of the giant magneto-impedance is improved by an order of magnitude. If this method is used for stress impedance, it will also have a higher sensitivity. The existing methods of studying the giant stress impedance effect (GSI) [5] obtain low stress impedance effect [6], and the annealing methods are mainly temperature annealing, current annealing, magnetic field annealing and so on [7-10].

At present, there are few reports on the stress-impedance effect of Fe-based alloy ribbons with different heating rates. The longitudinal driving method will be used in this paper to test the GSI of

ISSN: 2414-1895 DOI: 10.6919/ICJE.202208_8(8).0032

Fe-based alloy thin strip samples annealed at various heating rates above the crystallization temperature(873.15K). Higher stress-impedance ratio and stress-impedance sensitivity were obtained, which has important guiding significance for the fabrication of stress sensors and other devices.

2. Experimental

A single-roll rapid quenching method was used to create Fe-based ($Fe_{73.5}Cu_1Nb_3Si_{13.5}B_9$) amorphous ribbons with a width of 0.50mm and a thickness of 38μm. For the annealing process, a thin strip sample with a length of 22cm was used. The strip sample chosen for the experiment has a uniform width and thickness and was annealed at 873.15K with nitrogen protection. Flowing nitrogen gas was introduced during annealing to prevent the sample from oxidizing. The three stages of annealing are as follows: the heating stage involves heating the samples from room temperature to 873.15K. The heat preservation stage involves maintaining the heat at 873.15K for 30min. In the experiment, the holding time and cooling time for every sample were kept constant; the only variable was the heating rate, which was changed to 0.12K/s-2.81K/s from room temperature to 873.15K.

Measure the stress-impedance curve of a thin strip of a Fe-based alloy in longitudinal drive mode using an HP4294A impedance analyzer, and then calculate the stress-impedance ratio as follows:

$$\frac{\Delta Z}{Z}=\frac{Z(\sigma_{ex})-Z(\sigma_{max})}{Z(\sigma_{max})}\times 100\% \tag{1}$$

where Z(σex) and Z(σmax) are the impedance values when the applied stress is any value and maximum value. The stress impedance sensitivity is defined as:

$$\xi=\frac{(\Delta Z/Z)_{max}}{\Delta H}\times 100\% \tag{2}$$

where (ΔZ/Z)max is the maximum stress-impedance ratio, and ΔH is the half-width of the closed stress-impedance curve.

3. Results and Discussion

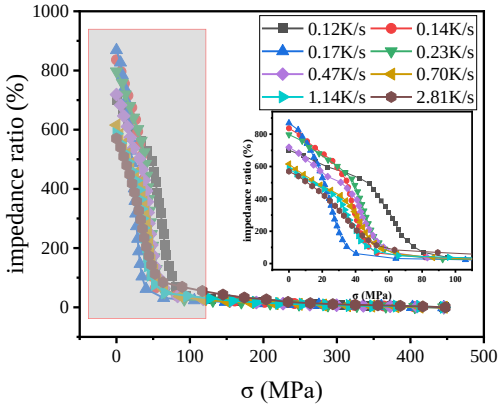

Figure 1. SI curves of different heating rates

Figure 1 shows the relationship between the stress-impedance ratio and the applied stress along the axis of the thin strip during 873.15K free annealing at 400kHz driving frequency. The heating rates are 0.12K/s, 0.14K/s, 0.17K/s, 0.23K/s, 0.47K/s, 0.70K/s, 1.41K/s, 2.81K/s, as shown in the figure,

ISSN: 2414-1895 DOI: 10.6919/ICJE.202208_8(8).0032

the maximum stress-impedance ratio of all samples is at 0MPa, and as stress increases, the stress-impedance ratio increases. The stress-impedance ratio has a good linear relationship with the stress in the range of 0MPa-90MPa. While in the range of 90MPa-450MPa, as stress increases, the material's stress-impedance ratio gradually decreases and tends to saturate to 0, and sensitivity is low.

Figure 2(a) shows the relationship between the maximum stress-impedance ratio and the heating rate of the sample in the SI characteristic curve. Maximum stress-to-resistance ratio rises with increasing heating rate between 0.12K/s and 0.17K/s, reaching its highest value of 868.65%. Maximum stress-impedance ratio of the material gradually falls with increasing heating rate between 0.17K/s and 2.81K/s. As can be seen, the stress impedance is quite low when the heating rate is sluggish. Figure 2(b) shows the relationship between the SI sensitivity of the sample and the heating rate. The heating rate is in the range of 0.12K/s-0.17K/s. With the increase of the heating rate, the SI sensitivity gradually increases. When the heating rate is 0.17K/s reaches the maximum value of 37.36%. When the heating rate is between 0.17K/s and 0.70K/s, the stress impedance sensitivity constantly declines with an increase in the heating rate, dropping from 37.36% to 15.37% and decreasing by around 2.4 times. It can be shown that the heating rate has a significant impact on the maximum stress-impedance ratio and sensitivity of the material after 0.70K/s, when the change in sensitivity is minimal and tends to be steady. After free annealing at 873.15K, the α-Fe(Si) nanocrystalline phase has a negative magnetostriction coefficient, whereas the untreated amorphous as-cast sample has a large positive magnetostriction coefficient. The different heating rates will affect the rate at which nanocrystals form in Fe-based alloys, resulting in different stress-impedance ratios of the materials.

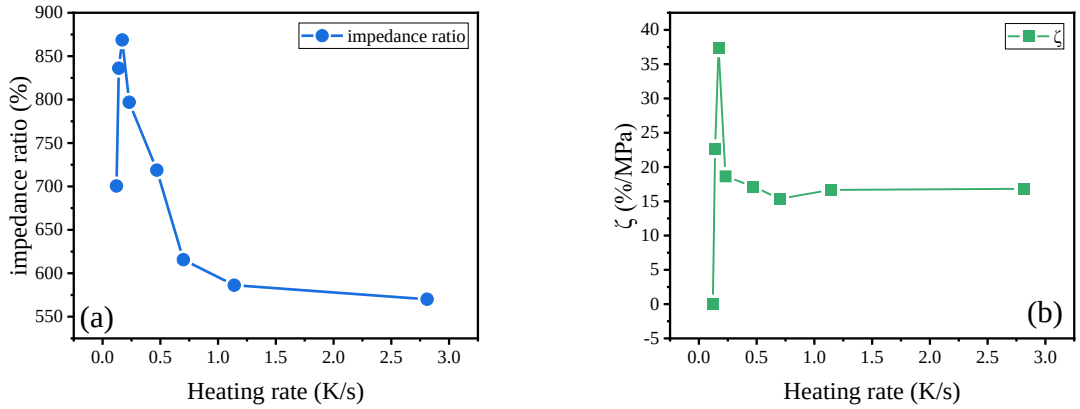

Figure 2. (a) The relationship between the maximum stress-impedance ratio and the heating rate; (b) The relationship between the stress-impedance sensitivity and the heating rate

According to the maximum stress-impedance ratio and stress-impedance sensitivity mentioned in Figure 2, three typical heating rates are selected for discussion. Figure 3 shows the relationship between stress-impedance ratio and stress at different frequencies. Figure 3(a)(b)(c) are samples annealed at heating rates of 0.12K/s, 0.17K/s and 2.81K/s, respectively. It can be seen that under different frequencies, the SI characteristic curves of the samples have obvious differences, and the maximum stress-impedance ratio is at 0MPa. With the increase of the applied stress, the stress-impedance ratio is at a small stress (0-85Mpa), its The change trend of the stress-impedance ratio is obvious and has a good linear trend. After 85Mpa, although the stress-impedance ratio has a good linear relationship with the applied stress, its change range is small.

ISSN: 2414-1895 DOI: 10.6919/ICJE.202208_8(8).0032

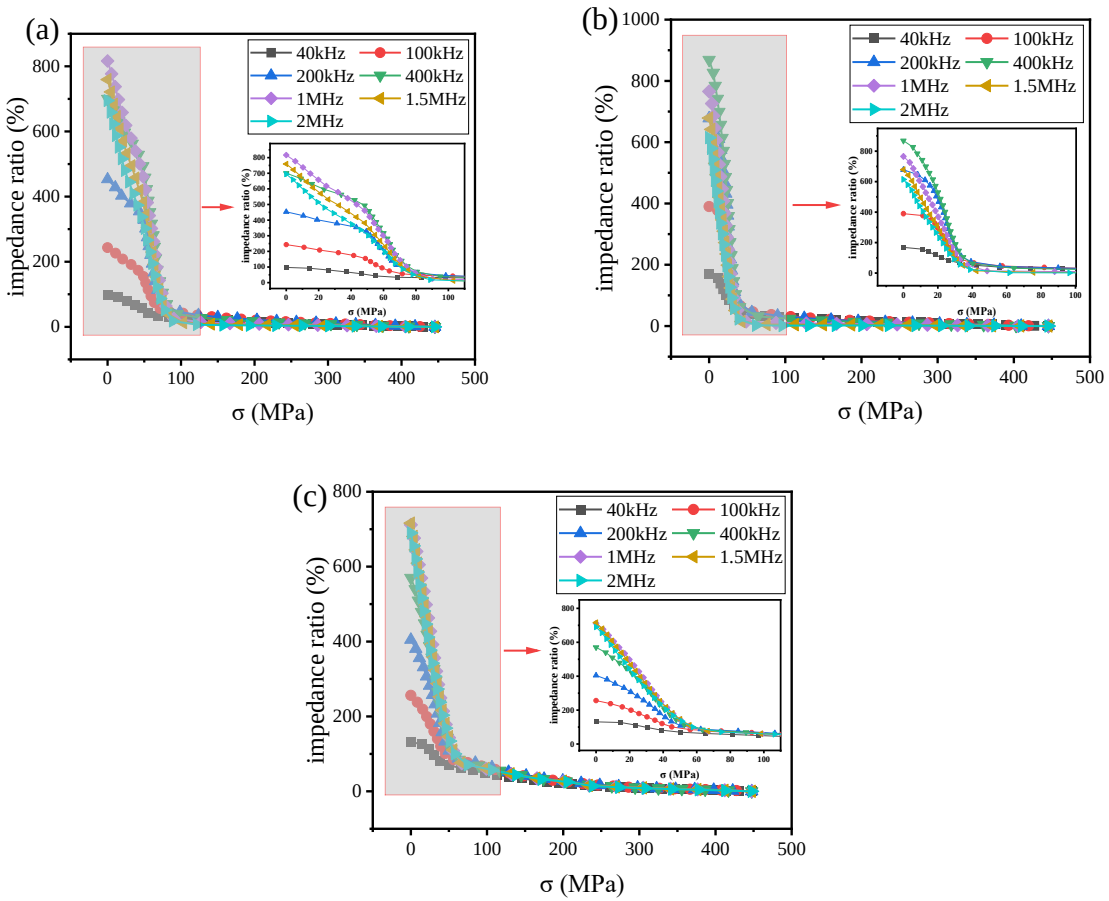

Figure 3. SI curves of samples with a heating rate of (a) 0.12K/s; (b) 0.17K/s; (c) 2.81K/s at different frequencies

By analyzing the data in Figure 3, the relationship between the maximum stress-impedance ratio and frequency of the sample in Figure 4(a) can be obtained. The test frequency range is 40kHz-2MHz. The figure shows that all three curves exhibit the same trend of change between 0-400kHz. The stress-impedance ratio gradually rises as the frequency rises. The stress impedance is significantly influenced by the frequency at 400kHz-2MHz, when the curve of the 0.17K/s heating rate declines linearly. The stress-impedance ratio is less impacted by frequency in curves with heating rates of 0.12K/s and 2.81K/s, which have a mild changing trend.

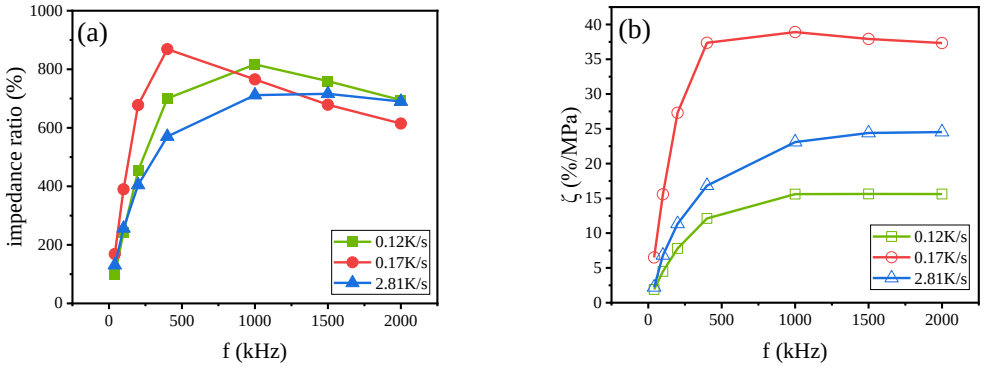

Figure 4. (a) The relationship between the maximum stress-impedance ratio and frequency; (b) the relationship between the stress-impedance sensitivity and frequency

ISSN: 2414-1895 DOI: 10.6919/ICJE.202208_8(8).0032

Figure 4(b) shows the relationship between stress impedance sensitivity and frequency. The figure shows that the sample's stress impedance sensitivity at a heating rate of 0.17K/s changes the most with frequency, while that of the sample at heating rates of 0.12K/s and 2.81K/s changes the least with frequency.

The magnetic permeability [11], magnetostriction coefficient, and skin effect of the material all influence the change trend of the SI effect. When the external stress along the axis of the thin strip acts on the thin strip during the SI test, the material has magnetostrictive properties [12]. Because of the close relationship between the magnetic domain mechanism in ferromagnets and the stress state, the position of the magnetic domain changes under stress, as does the direction of spontaneous magnetization. At the same time, the skin effect demonstrates that:

$$\delta=\sqrt{\frac{\rho}{\pi \bullet f \bullet \mu_0 \bullet \mu_r}} \tag{3}$$

where ρ is the resistivity of the material, f is the frequency of the current passed through the sample, μ0 is the magnetic permeability of the sample, and μr is the relative permeability. At a certain frequency, with the increase of the applied stress, the stress impedance effect decreases. The stress impedance of the Fe-based alloy strip after annealing changes obviously with the stress. The change of the inductance in the material causes the magnetic permeability to change. When the magnetic permeability is low, it results in a larger skin depth, which results in a lower impedance. Conversely, when the magnetic permeability is higher, the impedance is higher.

4. Conclusion

The Fe-based alloy samples obtained by free annealing at 873.15K, the GSI of the material can be significantly improved by using the longitudinal drive mode, and the heating rate will significantly affect the GSI of the material. Using a heating rate of 0.17K/s, thin strips of Fe-based alloy were annealed at 873.15K. The maximum stress-impedance ratio and stress-impedance sensitivity of the sample at 400kHz both have the highest value. The highest stress-impedance ratio is 868.65%, and its stress-response sensitivity can reach 37.36%/MPa. The impact of the nanocrystalline phase is crucial in explaining the performance disparity. Different device fabrication criteria can be met by applying the test results of samples heated at various rates under various pressures and frequencies.

Acknowledgments

Project supported by the Natural Science Foundation of China (52071165), Natural Science Foundation of Xinjiang Uygur Autonomous Region (2021D01B47), Open Research Fund of Key Laboratory of Solid State Optoelectronic Devices of Zhejiang Province (2020E010102), Tianshui Normal University high-level pre-research project (GJB2021-09).

References

[1] Y. Yoshizawa, S. Oguma, K. Yamauchi, New Fe-based soft magnetic alloys composed of ultrafine grain structure, Journal of Applied Physics, Vol. 64 (1988) No. 10, p. 6044-6046.

[2] Y. Yoshizawa, K. Yamauchi, Induced magnetic anisotropy and thickness dependence of magnetic properties in nanocrystalline alloy "finemet", J. Magn. Soc. Jpn., Vol. 14 (1990) No. 2, p. 193-196.

[3] Y. Yoshizawa, K. Yamauchi, Magnetic Properties of Nanocrystalline Fe-Based Soft Magnetic Alloys, MRS Proceedings, Vol. 232 (1991) No. 1, p. 183.

[4] J.X. Yang, X.L. Yang, G. Chen, A new type of longitudinal driving giant magneto-impedance effect, Chinese Science Bulleyin, Vol. 43 (1998) No. 10, p. 1051-1053. (In Chinese).

ISSN: 2414-1895 DOI: 10.6919/ICJE.202208_8(8).0032

[5] L.P. Shen, T. Uchiyama, K. Mohri, E. Kita, K. Bushida, Sensitive stress-impedance micro sensor using amorphous magnetostrictive wire, IEEE Transactions on Magnetics, Vol. 33 (1997) No. 5, p. 3355-3357.

[6] D.A. Bukreev, M.S. Derevyanko, A.A. Moiseev, A.V. Semirov, P.A. Savin, G.V. Kurlyandskaya, Magnetoimpedance and Stress-Impedance Effects in Amorphous CoFeSiB Ribbons at Elevated Temperatures, Materials, Vol. 13 (2020) No. 14, p. 3216.

[7] H. Wei, D. Li, Z. Lu, S. Zhou, H. Zhang, Giant stress-impedance effect in amorphous and current annealed Fe73.5Cu1Nb3Si13.5B9 wires, Journal of Magnetism and Magnetic Materials, Vol. 239 (2002) No. 1-3, p. 567-569.

[8] D. Li, Z. Lu, S. Zhou, Giant stress-impedance effect in amorphous and thermally annealed Fe73.5Cu1Nb3Si13.5B9 ribbons, Sensors and Actuators A: Physical, Vol. 109 (2003) No. 1-2, p. 68-71.

[9] Z. Chen, D. Li, Z. Lu, S. Zhou, Giant Stress-Impedance Effect in Co71.8Fe4.9Nb0.8Si7.5B15 Glass Covered Amorphous Wires, J. Iron Steel Res. Int., Vol. 13 (2006) No. 4, p. 49-50.

[10] D.G. Jiang, H.D. Li, Z.H. Zhu, Influence of annealing condition on the stress impedance of Fe-based amorphous alloy ribbons, Rare Metal Materials and Engineering, Vol. 31 (2008) No. 1, p. 33-35. (In Chinese).

[11] A. Ostaszewska-Liżewska, R. Szewczyk, P. Raback, M. Malinen, Modelling the Characteristics of Ring-Shaped Magnetoelastic Force Sensor in Mohri's Configuration, Sensors., Vol. 20 (2020) No. 1, p. 266.

[12] G. Herzer, Magnetic field-induced anisotropy in nanocrystalline Fe-Cu-Nb-Si-B alloys, Journal of Magnetism and Magnetic Materials, Vol. 133 (1994) No. 1-3, p. 248-250.